


**Please cite the Published Version**

Li, Zhen, Meng, Zhaozong, Soutis, Constantinos, Haigh, Arthur, Wang, Ping and Gibson, Andrew  (2022) Bimodal microwave method for thickness estimation of surface coatings on polymer composites. *Advanced Engineering Materials*, 24 (5). p. 2100494. ISSN 1438-1656

**DOI:** <https://doi.org/10.1002/adem.202100494>

**Publisher:** Wiley

**Version:** Accepted Version

**Downloaded from:** <https://e-space.mmu.ac.uk/629881/>

**Additional Information:** This is the peer reviewed version of the following article: Li, Z., Meng, Z., Soutis, C., Haigh, A., Wang, P. and Gibson, A. (2022), Bimodal Microwave Method for Thickness Estimation of Surface Coatings on Polymer Composites. *Adv. Eng. Mater.*, 24: 2100494., which has been published in final form at <https://doi.org/10.1002/adem.202100494>. This article may be used for non-commercial purposes in accordance with Wiley Terms and Conditions for Use of Self-Archived Versions. This article may not be enhanced, enriched or otherwise transformed into a derivative work, without express permission from Wiley or by statutory rights under applicable legislation. Copyright notices must not be removed, obscured or modified. The article must be linked to Wiley's version of record on Wiley Online Library and any embedding, framing or otherwise making available the article or pages thereof by third parties from platforms, services and websites other than Wiley Online Library must be prohibited.

**Enquiries:**

If you have questions about this document, contact [openresearch@mmu.ac.uk](mailto:openresearch@mmu.ac.uk). Please include the URL of the record in e-space. If you believe that your, or a third party's rights have been compromised through this document please see our Take Down policy (available from <https://www.mmu.ac.uk/library/using-the-library/policies-and-guidelines>)

**Bimodal Microwave Method for Thickness Estimation of  
Surface Coatings on Polymer Composites**

*Zhen Li\**, *Zhaozong Meng*, *Constantinos Soutis*, *Arthur Haigh*, *Ping Wang*, *Andrew Gibson*

Dr. Zhen Li, Prof. Ping Wang

College of Automation Engineering

Nanjing University of Aeronautics and Astronautics

Nanjing, 211106, China

Email: [zhenli@nuaa.edu.cn](mailto:zhenli@nuaa.edu.cn)

Dr. Zhaozong Meng

School of Mechanical Engineering

Hebei University of Technology

Tianjin, 300130, China

Prof. Constantinos Soutis, Dr. Arthur Haigh

Aerospace Research Institute

The University of Manchester

Manchester, M13 9PL, UK

Prof. Andrew Gibson

Faculty of Science and Engineering

Manchester Metropolitan University

Manchester, M1 5GD, UK

Keywords: composites, coating thickness, microwave sensors, electromagnetic field

## Abstract

Two new microwave sensors, an open cylindrical cavity resonator with a T-shaped excitation element and a flanged coaxial line sensor, are used for the non-destructive thickness measurement of surface coatings on a unidirectional carbon fibre-reinforced polymer (CFRP) laminate. Both sensors are found insensitive to the anisotropy of the composite substrate, offering easy implementation. Three commercially available plastic films, polyethylene (PE), polyethylene terephthalate (PET) and polyvinyl chloride (PVC) are used to simulate the coating. In the setup, the microwave sensors are directly mounted on the 4 mm thick composite plate. The coating affects the surface impedance of the composite, causing changes to the signal reflection. Calibration is performed by the measurement of samples with known coating thicknesses. For the cavity resonator, a linear relationship is obtained between the resonance frequency shift and the thickness; the difference between the measured and actual thickness values is around 17  $\mu\text{m}$ . For the coaxial line sensor, the phase variation increases with increasing thickness. For both sensors used, the estimation error for a coating thickness in the region of 200  $\mu\text{m}$  is well within 10%.

## 1. Introduction

The surfaces of an aeroplane are commonly painted for decorative and functional purposes, e.g., minimisation of aerodynamic drag, resistance to chemicals and protection from erosion, extreme thermal cycles and high levels of ultraviolet exposure. The coating should be thick enough for these functions, while it cannot be too thick to increase the weight, reducing the aircraft performance, fuel efficiency and lightning protection<sup>[1]</sup>. The painting process is mostly done manually, so **the evenness of the coating cannot be guaranteed and** a high level of thickness variation can be found <sup>[2]</sup>. **Repainting is required when the coating is excessively thick.** Conventionally, the thickness is checked by weight measurement, which

can lead to an unwanted cycle delay of few days and pose difficulties for large components. Local thickness information cannot be obtained by this approach either. For better quality control and inspection, non-destructive measurement methods can be utilised, such as ultrasonics<sup>[3]</sup>, terahertz scanning<sup>[4]</sup>, guided waves<sup>[5]</sup> and eddy current testing<sup>[6]</sup>. However, each method has its limitations and specific ranges of applicability. For example, ultrasonic testing usually needs couplants (e.g., water or gel) and is accurate for very thick coatings. The terahertz equipment is intricate and not suitable for on-site tests. For guided waves, transducers should be permanently bonded on the surface. The eddy current testing is mostly applied to high-conductivity substrates like metals, where strong currents can be induced. However, carbon fibre-reinforced polymer (CFRP) composites that are increasingly used in aircraft have relatively low electrical conductivities<sup>[7]</sup>. There is a great demand for a sensor that can be readily used for thin coatings on CFRP.

In recent years, microwave testing as an emerging technique has received considerable interest<sup>[8]–[10]</sup>. The microwave methods have the advantages of no need for couplants or transducers, easy experimental setup and low signal power consumption. In terms of coating thickness measurement, some preliminary research was conducted using open cylindrical cavity resonators and rectangular waveguides. Takeuchi et al.<sup>[11]</sup> developed a cavity resonator and chose the  $TM_{011}$  mode resonance frequency as a thickness indicator. Coated composite panels were measured with the thickness ranging from 50.8  $\mu\text{m}$  to 203.2  $\mu\text{m}$ . Using the fitting equation from calibration, the results agreed well with those by a commercial instrument following the standard wedge cut method (a destructive approach). Hinken<sup>[12]</sup> designed a  $TE_{012}$  mode cavity and calibrated with one type of plastic foil. For each of the three substrates (i.e., CFRP, a copper sheet and CFRP with copper mesh), a calibration curve was generated by five points, covering the thickness from 0 to 400  $\mu\text{m}$  with an interval of 100  $\mu\text{m}$ . The

thickness of a new sample could be estimated from the calibration data. In both references, the information about the CFRP type (e.g., unidirectional (UD), multi-directional or woven) and the designs of the sensors were not provided.

Zoughi et al. <sup>[13]</sup> applied an open-ended X-band (8-12 GHz) rectangular waveguide to measure coatings on a woven composite substrate. Three dielectrics, i.e., 1.69 mm garolite fiberglass-epoxy, 5.35 mm polyethylene (PE) and 1.28 mm nylon sheets, were used to simulate the coating. An analytical model was employed to compute the thickness from the reflection coefficients, and the estimation errors were within 15 %. The composite plate was shown electrically isotropic due to the woven structure. In comparison, UD CFRP is more conductive along the fibres. As the electric field in the waveguide is parallel to the narrow dimension, the portion of the signal reflection is strongly associated with the angle between that dimension and the fibre orientation <sup>[14]</sup>. Therefore, special attention should be paid to when the waveguide approach is used for UD CFRP. The positioning of the waveguide in the measurement should be kept the same as that in the calibration.

In the present work, an open cylindrical cavity resonator with simple excitation and a flanged coaxial line sensor are proposed. Special probe placement with respect to the fibre orientation of the CFRP substrate is not needed due to the symmetric electric fields generated. The sensor design and related detection principles are presented in detail. The anisotropy of a UD CFRP plate is examined first using an X-band waveguide. Three types of dielectric foils are used as coatings for calibration. The effect of the coating thickness on the signal response over a wide frequency range is investigated, and the frequency that can provide the optimal performance is analysed. The accuracy of the thickness measurement is studied to show the sensors' effectiveness.

## 2. Materials and methods

### 2.1. Cavity resonator sensor

The diagram of the cavity resonator sensor is illustrated in Figure 1. The open cavity consists of a cylindrical wall and an endplate. The radius of the cavity ( $r$ ) is 46 mm, and the height ( $h$ ) is 40 mm. A SubMiniature version A (SMA) connector was mounted on the endplate for power transfer. The inner conductor of the connector was extended 2 mm out of the endplate and soldered to a 35 mm long copper wire. The extended conductor and the horizontal bar produce a T-shaped projecting structure for resonance excitation: the former can induce transverse magnetic ( $TM_{nml}$ ) modes and the latter can excite both TM and transverse electric ( $TE_{nml}$ ) modes. TM and TE modes mean that the magnetic and electric fields only exist in the plane transverse to the axis of the cylinder, respectively<sup>[15]</sup>. Subscript  $n$  is the number of full-period variations along the circumference of the cylinder,  $m$  is the number of zeros of the field intensity in the radial direction, and  $l$  is the number of half-period variations along the axial direction. The resonance frequencies of the  $TM_{nml}$  and  $TE_{nml}$  modes in an air-filled closed cylindrical cavity can be computed by

$$f_{TM_{nml}} = \frac{c}{2\pi} \sqrt{\left(\frac{p_{nm}}{r}\right)^2 + \left(\frac{l\pi}{h}\right)^2} \quad (1a)$$

$$f_{TE_{nml}} = \frac{c}{2\pi} \sqrt{\left(\frac{p'_{nm}}{r}\right)^2 + \left(\frac{l\pi}{h}\right)^2} \quad (1b)$$

where  $c$  is the speed of light in free space.  $p_{nm}$  is the  $m$ -th root of the Bessel function of first kind  $J_n$ , and  $p'_{nm}$  is the  $m$ -th root of the derivative of  $J_n$ .

In the test, the sensor and the composite form a closed cavity. When a coating layer is introduced on top of the composite, the surface impedance becomes a function of the coating thickness and electrical properties of both coating and CFRP. The effective surface impedance

increases with increasing coating thickness. According to the perturbation theory, the increase of the surface impedance can result in a smaller resonance frequency and a lower quality factor due to more dielectric and radiation loss.

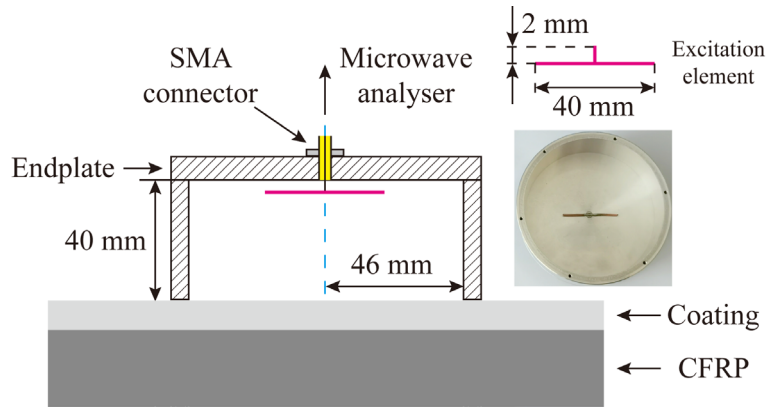


Figure 1 Schematic diagram of the open cavity resonator

## 2.2. Coaxial line probe

The structure of the open coaxial line sensor is presented in Figure 2, where the electromagnetic fields in the line are rotationally symmetric. The outer conductor of a conventional coaxial line probe for permittivity characterisation generally has a small outer diameter (less than 20 mm) [16]. Here a large aluminium flange was made with an outer diameter of 80 mm, so the sensor can be easily placed on a surface. A SMA connector was also used for signal feed.

Well-established analytical modelling of radiation from an open-ended coaxial line into stratified dielectrics can be found in the literature. The present setup can be approximated by one of the models where a dielectric sample is backed by an infinitely large medium [17]. Microwave signals have low penetration in conductive composites [14]. Thus, the thickness of the composite used is electrically large and can be viewed as infinity in that regard. The reflection coefficient  $\Gamma$  at the aperture can be expressed as

$$\Gamma = \frac{1-y}{1+y} \quad (2a)$$

$$y = \frac{\varepsilon_{r1}}{\sqrt{\varepsilon_{rc}} \ln(b/a)} \int_0^\infty \frac{[J_0(k_0 \zeta b) - J_0(k_0 \zeta a)]^2}{\zeta} F(\zeta) d\zeta \quad (2b)$$

where  $\varepsilon_{r1}$  is the relative permittivity of the coating layer.  $\varepsilon_{rc}$  is the relative permittivity of the dielectric (i.e., Teflon) in the coaxial line.  $a$  and  $b$  are the inner and outer radii of the Teflon ring, respectively. For the present sensor,  $a=0.65$  mm and  $b=2.05$  mm.  $J_0$  is the zero-order Bessel function of first kind.  $k_0=\omega/c$  is the free-space wavenumber, and  $\omega$  is the angular frequency. The function  $F(\zeta)$  associated with the boundary conditions can be given by

$$F(\zeta) = \frac{\varepsilon_{r2} \sqrt{\varepsilon_{r1} - \zeta^2} + j \varepsilon_{r1} \sqrt{\varepsilon_{r2} - \zeta^2} \tan(k_0 d \sqrt{\varepsilon_{r1} - \zeta^2})}{\varepsilon_{r1} \sqrt{\varepsilon_{r1} - \zeta^2} \sqrt{\varepsilon_{r2} - \zeta^2} + j \varepsilon_{r2} (\varepsilon_{r1} - \zeta^2) \tan(k_0 d \sqrt{\varepsilon_{r1} - \zeta^2})} \quad (3)$$

where  $d$  is the coating thickness and  $\varepsilon_{r2}$  is the relative permittivity of the composite.

As indicated in Equations (2) and (3), it is not straightforward to retrieve the thickness from the analytical model. It should be noted that the reference plane of the complex reflection coefficient  $S_{11}$  acquired from the analyser may not be exactly at the aperture where  $\Gamma$  is defined. Hence, appropriate correction is needed, further exacerbating the thickness determination. Here a simple calibration approach is adopted by recording the signals for different coatings. For a new signal, the thickness can be interpolated from the calibration curve produced for the specific material.

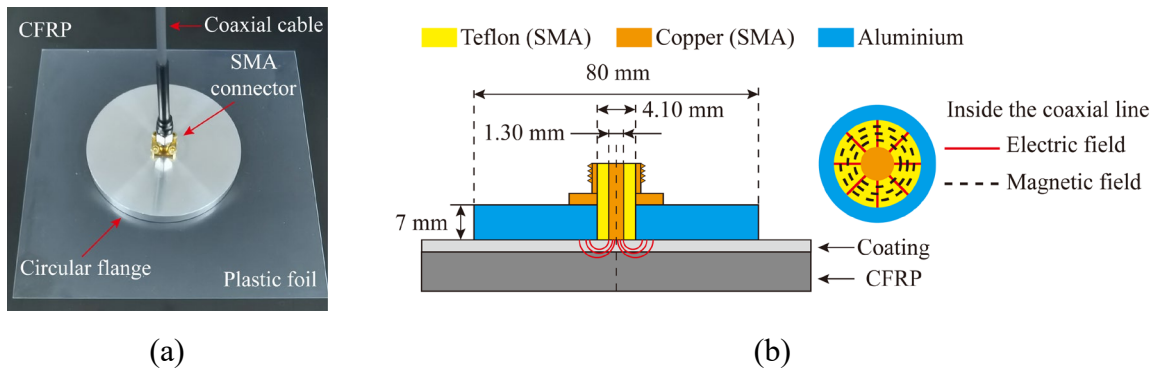


Figure 2 Open coaxial line sensor for coating thickness measurement: (a) photograph; (b) schematic diagram of the setup (not to scale)



### 2.3. Experimental setup

The signals for the two sensors were generated by a Fieldfox N9951A portable microwave analyser (Keysight Technologies, Santa Rosa, CA), **and the sensor was connected to the analyser by a coaxial cable. A factory calibration known as CalReady was performed at the test port connector (i.e., Port 1).** For both sensors are one-port devices, only the  $S_{11}$  data were collected from the analyser by a LAN cable. The power of the signal was set to -15 dBm (i.e., 0.032 mW), **which was too low to cause any heating effect.** Three commercially available plastic films, PE, polyethylene terephthalate (PET) and polyvinyl chloride (PVC), were used to simulate the coating and placed on a 4 mm **thick** UD T300 CFRP laminate. **The measurement of thin dielectric layers is common practice in the calibration of a new coating thickness sensor, as an even surface can be provided.** The permittivity values of PE, PET and PVC at 3 GHz are  $2.25-j6.75 \times 10^{-4}$  [18],  $2.87-j2.74 \times 10^{-2}$  [19] and  $2.84-j1.57 \times 10^{-2}$  [18], respectively. Due to the low-loss characteristic, the permittivity values of these materials do not significantly change in the GHz range. For a single layer, the thicknesses of PE, PET and PVC **measured by a digital calliper (Pro's Kit co. Ltd., Shanghai, China)** were approximately 40  $\mu\text{m}$ , 50  $\mu\text{m}$  and 280  $\mu\text{m}$ , respectively. For PE and PET, up to 25 layers were tested with the maximum thickness over 1 mm, **same as typical aircraft painting.** For PVC, due to the larger layer thickness, up to seven layers were tested. Plastic pieces with dimensions of 150 mm $\times$ 120 mm (**larger than the probe aperture**) were cut and stacked onto the composite. The sensor was gently pressed against the films to eliminate air gaps between the foils. Three consecutive measurements were taken for each thickness case.

**A commercial eddy current technique-based coating thickness gauge (Uni-Trend Technology Co., Ltd, Dongguan, China) was also employed. When the gauge was**

directly placed on the composite, no indication of the thickness was given, showing the inapplicability.

### 3. Results and discussion

#### 3.1. Material anisotropy of UD CFRP

The signal responses at five angles ( $\theta$ ) between the electric field inside the waveguide and the fibres, i.e.,  $0^\circ$ ,  $30^\circ$ ,  $45^\circ$ ,  $60^\circ$  and  $90^\circ$ , are shown in Figure 3, where the curves do not overlap.

For the case where the electric field is parallel to the fibres (i.e.,  $\theta=0^\circ$ ), the energy reflected is the highest as would be expected. The maximum magnitude difference between the  $0^\circ$  and  $90^\circ$  cases is approximately 10%, confirming that the electrical conductivity of the composite plate is not homogeneous and the waveguide approach could not be applied for the measurement of coated UD CFRP. In comparison, the reflection coefficients were hardly changed when the two microwave sensors designed were rotated on the composite.

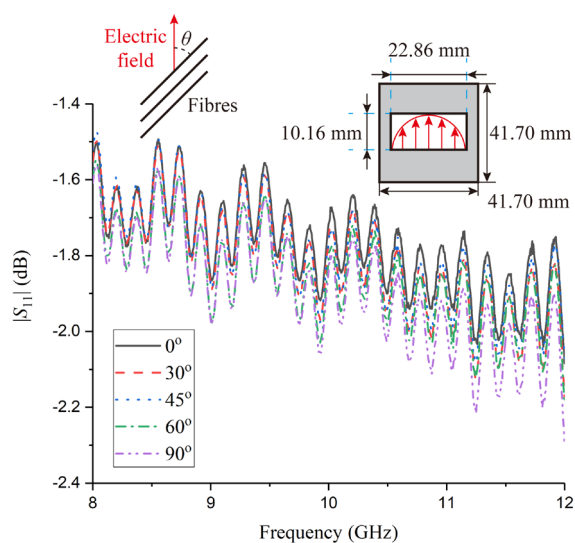


Figure 3 Reflectivity measurement of the composite with the waveguide placed at different angles

#### 3.2. Cavity resonator

Over a wide frequency range, a number of resonances can be excited in a closed cavity. As reported in the literature <sup>[20]</sup>, the fundamental mode  $TM_{010}$  has the lowest resonance frequency (around 2.49 GHz for the cavity designed) and quality factor, so higher modes are of interest

here. The reflection coefficients for the composite plate over a frequency range of 4-10 GHz are presented in Figure 4, where more modes exist at higher frequencies and the difference between adjacent resonance frequencies becomes smaller. To avoid interference and increased fabrication cost of the microwave circuit at high frequencies, two low resonance frequencies (i.e., 4.495 GHz and 4.893 GHz) are chosen for further analysis. 4.495 GHz corresponds to the frequency in the  $TM_{011}$  mode (denoted by  $f_{r1}$ ), while 4.893 GHz corresponds to the frequency in the  $TE_{211}$  mode (denoted by  $f_{r2}$ ). The real resonance frequency of each mode is slightly lower than the ideal one (i.e., 4.502 GHz for the  $TM_{011}$  mode and 4.907 GHz for the  $TE_{211}$  mode), as the electrical conductivity of the composite is lower than that of a perfect conductor. Detailed field distributions of the two modes can be referred to in [21].

The shifts of the two frequencies with respect to the total thickness of the stacked dielectric layers  $d$  are shown in Figure 5, where the frequency decreases with increasing thickness and linear trends are observed. The relationship between the resonance frequency and coating thickness is obtained using regression analysis.

$$f_{r1} = k_1 d + c_1 \quad (4a)$$

$$f_{r2} = k_2 d + c_2 \quad (4b)$$

where  $k_1$ ,  $k_2$ ,  $c_1$  and  $c_2$  are the regression constants, and the values obtained are listed in Table 1. The high coefficients of determination imply good fitting. For each mode, the regression constants for the three coating materials are similar, suggesting that the frequency change is independent of the material. The average measurement sensitivities using  $f_{r1}$  and  $f_{r2}$  are around 81.95 kHz/ $\mu\text{m}$  and 64.18 kHz/ $\mu\text{m}$ , respectively. The standard deviation of the frequency measurement is up to 1.25 MHz, so the minimum thickness differences that can be detected from the  $f_{r1}$  and  $f_{r2}$  measurements are 16.81  $\mu\text{m}$  and 20.15  $\mu\text{m}$ , respectively. Therefore, the estimation error can be well below 10 % when  $d$  is larger than 200  $\mu\text{m}$ .

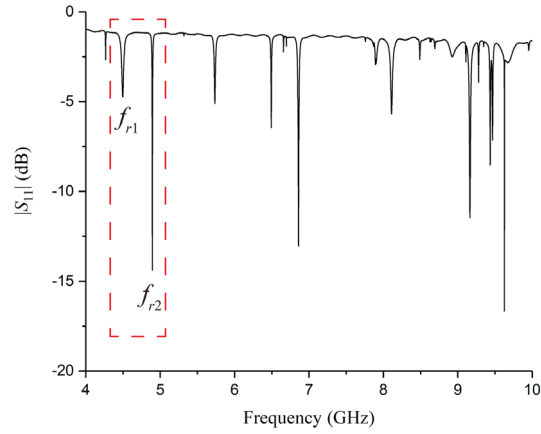


Figure 4 Response of the resonant cavity for the composite plate in terms of reflection coefficient versus frequency

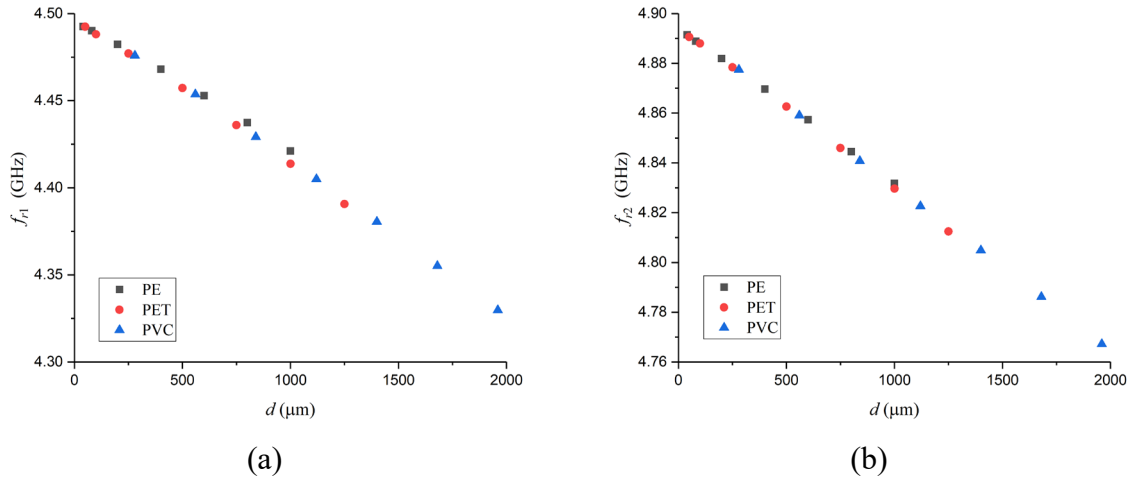


Figure 5 Variation of resonance frequency with respect to total thickness ( $d$ ) of the stacked dielectric layers on the composite: (a) resonance frequency of the  $TM_{011}$  mode,  $f_{r1}$ ; (b) resonance frequency of the  $TE_{211}$  mode,  $f_{r2}$

Table 1 Regression constants and coefficients of determination ( $R^2$ ) in Equations (4a) and (4b)

	PE	PET	PVC
$k_1$	$-7.436 \times 10^{-5}$	$-8.421 \times 10^{-5}$	$-8.728 \times 10^{-5}$
$c_1$	4.497	4.498	4.502
$R^2$ (4a)	0.9988	0.9989	0.9997
$k_2$	$-6.205 \times 10^{-5}$	$-6.514 \times 10^{-5}$	$-6.536 \times 10^{-5}$
$c_2$	4.894	4.895	4.896
$R^2$ (4b)	0.9998	0.9997	0.9999

For the fitting functions obtained, the independence of the coating material is examined with thin Flame Retardant 4 (FR4) woven fiberglass-epoxy sheets (typical  $\epsilon_r$  of  $4.32-j0.10$ ), which are also readily available. Five FR4 samples with thicknesses of 0.15 mm, 0.35 mm, 0.45 mm, 0.71 mm and 0.80 mm were separately placed on the CFRP plate. The average  $k_1$ ,  $k_2$ ,  $c_1$  and  $c_2$  in Table 1 are used for the prediction of the resonance frequency. As presented in Figure 6, for both  $f_{r1}$  and  $f_{r2}$ , good agreement is seen between the tests and the estimation, and especially a better fit is observed in  $f_{r2}$ . Hence, the TE<sub>211</sub> mode resonance frequency could be potentially used for a wide range of dielectrics.

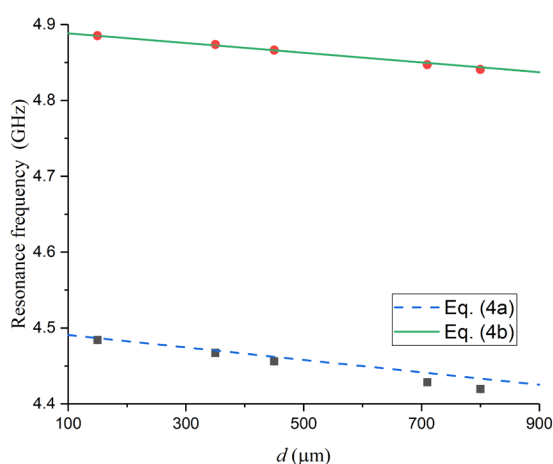


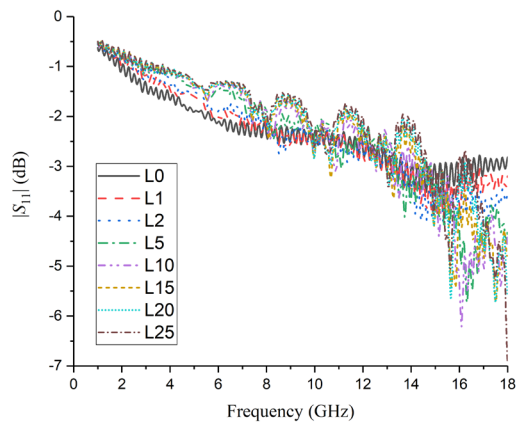
Figure 6 Comparison between the measured and predicted resonance frequencies for a fiberglass-epoxy coating using the fitting functions from the calibration

### 3.3. Open-ended coaxial probe

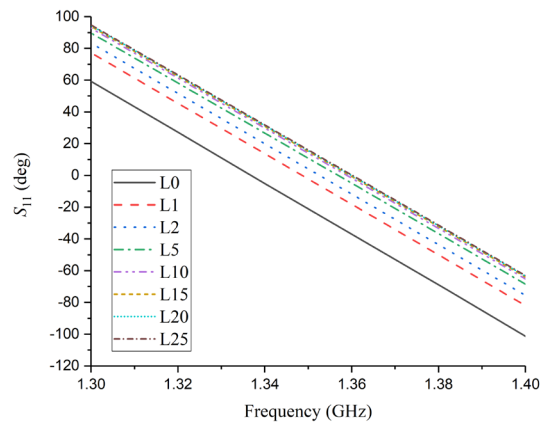
The coaxial probe was first used to measure the PE layers. As given in Figure 7 (a), over the whole frequency range from 1 GHz to 18 GHz, there is no pattern between the magnitude variation and the thickness change. **In terms of the phase**, in Figure 7 (b), **the curves for different thicknesses** over 1.30-1.40 GHz show that **at an arbitrary frequency** the phase increases with increasing thickness and gradually stabilises, **demonstrating a good correlation**. The phase curves over the full frequency range are not presented here, as they are closely spaced and cannot be readily differentiated. At nine selected frequencies, the phase

variations with respect to the reference case of CFRP only are shown in Figure 7 (c), where the largest dynamic changes are observed at 16 GHz. This frequency is also used in the analysis of the PET and PVC cases. As demonstrated in Figure 8, at thickness  $d$  below 250  $\mu\text{m}$  the phase differences between the three foil cases are small. The PET and PVC curves overlap for the similar dielectric properties, and at  $d \geq 250 \mu\text{m}$  the phase changes are lower than those of PE.

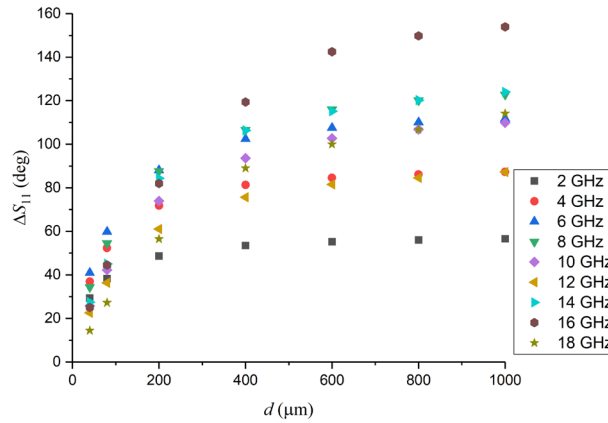
Polynomials can be introduced to fit the points, and the monotonic characteristic of the fitted curves suggests that they can be employed for the thickness determination. A high estimation accuracy with an error of less than 10% can be achieved at thicknesses below 500  $\mu\text{m}$  **due to the high rates of change. Taking the fitted function of PET as an example (i.e.,  $S_{11} = 7.9129 \times 10^{-14} d^5 - 4.6959 \times 10^{-10} d^4 + 1.0338 \times 10^{-6} d^3 - 1.0874 \times 10^{-3} d^2 + 0.5789d + 0.8745$ ), given the phase value  $93.51^\circ$  at 250 mm, the thickness estimated is 257.48 mm, which corresponds to an error of 2.99%.**



(a)



(b)



(c)

Figure 7 Signal response of the PE coating using the coaxial line sensor developed (each case is represented by ‘L+number of layer’): (a) magnitude of  $S_{11}$  over 1-18 GHz; (b) phase of  $S_{11}$  over 1.30-1.40 GHz; (c) phase differences between the coating and non-coating cases at nine selected frequencies from 2 GHz to 18 GHz

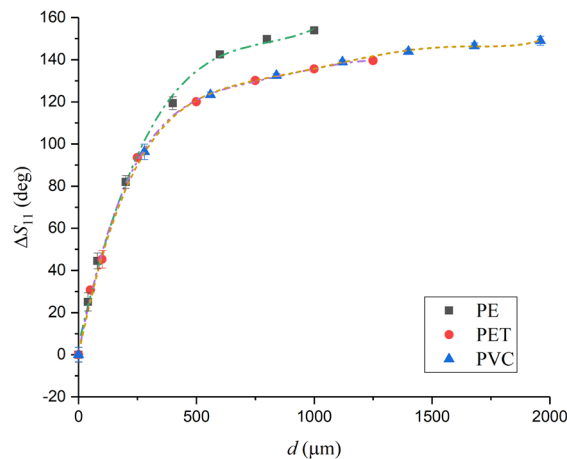


Figure 8 Relationship between the phase response and the total thickness for the three coating materials at 16 GHz (the standard deviations of the data points are also provided)

#### 4. Concluding remarks

Two new microwave sensors have been developed for the thickness measurement of dielectric coatings on unidirectional CFRP plates. The sensors can be positioned without the need to consider the anisotropy of the composite. In terms of measurement accuracy, the two sensors complement each other: the cavity resonator sensor is more suitable for relatively thick coatings, while the coaxial line sensor better suits thin coatings. For the cavity sensor, a linear

relationship exists between the resonance frequency and coating thickness. It is suggested that the sensor can be employed for materials that are not used in the calibration. For the coaxial sensor, a monotonic relationship can be established between the phase shift and coating thickness. In near future work, the effectiveness of the two sensors for more realistic coated composites will be explored, like painted surfaces.

### Acknowledgements

This work was financially supported by the Natural Science Foundation of Jiangsu Province (Grant No. BK20200427), the Shuangchuang Project of Jiangsu Province (Grant No. KFR20020) and the Fundamental Research Funds for the Central Universities (Grant No. NS2020019). Special thanks to Dr. Changcheng Wu and Dr. Fei Fei for assistance in the experiments.

### References

- [1] F. Moupfouma, *SAE Int. J. Aerosp.* **2013**, 6, 2013.
- [2] FAA(Federal Aviation Administration), *Airframe Volume I*, United States Department Of Transportation, Oklahoma City, OK **2018**.
- [3] B. Pant, S.R. Skinner, J.E. Steck, *IEEE Trans. Instrum. Meas.* **2006**, 55, 1720.
- [4] K.-H.H. Im, I.-Y.Y. Yang, S.-K.K. Kim, J.-A.A. Jung, Y.-T.T. Cho, Y.-D.D. Woo, *J. Mech. Sci. Technol.* **2016**, 30, 4413.
- [5] P.-C. Ostiguy, N. Quaegebeur, P. Masson, *NDT E Int.* **2015**, 76, 17.
- [6] W. Yin, A.J. Peyton, *NDT E Int.* **2007**, 40, 43.
- [7] C. Soutis, *Prog. Aerosp. Sci.* **2005**, 41, 143.
- [8] Z. Li, P. Wang, A. Haigh, C. Soutis, A. Gibson, *Aeronaut. J.* **2021**, 125, 151.
- [9] K. Brinker, M. Dvorsky, M.T. Al Qaseer, R. Zoughi, *Philos. Trans. R. Soc. A Math. Phys. Eng. Sci.* **2020**, 378, 20190585.



- [10] Z. Li, A. Haigh, C. Soutis, A. Gibson, *Appl. Compos. Mater.* **2018**, 25, 965.
- [11] J.S. Takeuchi, M. Perque, P. Anderson, E.G. Sergoyan, *Microwave Paint Thickness Sensor*, **2011**, US 7898265.
- [12] J. Hinken, *Device for Measuring Coating Thickness*, **2016**, US 9395172.
- [13] R. Zoughi, J.R. Gallion, M.T. Ghasr, *IEEE Trans. Instrum. Meas.* **2016**, 65, 951.
- [14] Z. Li, A. Haigh, C. Soutis, A. Gibson, *Compos. Struct.* **2019**, 208, 224.
- [15] K.Q. Zhang, D.J. Li, *Electromagnetic Theory for Microwaves and Optoelectronics*, Springer, Ltd, Berlin, Germany **2008**.
- [16] T.P. Marsland, S. Evans, *IEE Proc. H Microwaves, Antennas Propag.* **1987**, 134, 341.
- [17] S.I. Ganchev, N. Qaddoumi, S. Bakhtiari, R. Zoughi, *IEEE Trans. Instrum. Meas.* **1995**, 44, 1023.
- [18] A.R. Von Hippel, *Dielectric Materials and Applications*, Artech House, New York **1995**.
- [19] J. Zechmeister, J. Lacik, in *2019 Conf. Microw. Tech.*, IEEE**2019**, 1.
- [20] D.M. Pozar, *Microwave Engineering*, John Wiley & Sons, New York **2012**.
- [21] J.A. Cuenca, *Characterisation of Powders Using Microwave Cavity Perturbation*, Cardiff University, **2016**.

The thickness of surface coating on unidirectional carbon fiber-reinforced polymer composites is measured with two new microwave sensors. From the experiments, good correlation is found between the coating thickness and the parameter of interest (i.e., the resonance frequency for the open cavity resonator sensor and phase for the coaxial line sensor).

Zhen Li\*, Zhaozong Meng, Constantinos Soutis, Arthur Haigh, Ping Wang, Andrew Gibson

### Bimodal Microwave Method for Thickness Estimation of Surface Coatings on Polymer Composites

